

RESEARCH ARTICLE

10.1002/2014JD022560

Key Points:

- A new data set of homogenized Italian sunshine duration records has been set up
- Sunshine duration temporal evolution has been studied for the period 1936–2013
- Results are discussed on the basis of total cloud cover temporal evolution

Correspondence to:

V. Manara,
veronica.manara@unimi.it

Citation:

Manara, V., M. C. Beltrano, M. Brunetti, M. Maugeri, A. Sanchez-Lorenzo, C. Simolo, and S. Sorrenti (2015), Sunshine duration variability and trends in Italy from homogenized instrumental time series (1936–2013), *J. Geophys. Res. Atmos.*, 120, 3622–3641, doi:10.1002/2014JD022560.

Received 10 SEP 2014

Accepted 27 MAR 2015

Accepted article online 21 APR 2015

Published online 5 MAY 2015

Sunshine duration variability and trends in Italy from homogenized instrumental time series (1936–2013)

Veronica Manara¹, Maria Carmen Beltrano², Michele Brunetti³, Maurizio Maugeri^{1,3}, Arturo Sanchez-Lorenzo^{4,5}, Claudia Simolo³, and Simona Sorrenti²

¹Department of Physics, Università degli Studi di Milano, Milan, Italy, ²Unità di Ricerca per la Climatologia e la Meteorologia applicate all'Agricoltura, Consiglio per la Ricerca e la Sperimentazione in Agricoltura, Rome, Italy, ³Institute of Atmospheric Sciences and Climate, CNR, Bologna, Italy, ⁴Department of Physics, University of Girona, Girona, Spain, ⁵Instituto Pirenaico de Ecología, Consejo Superior de Investigaciones Científicas, Zaragoza, Spain

Abstract A data set of quality checked daily sunshine duration measurements was collected from 104 Italian sites over the 1936 to 2013 period. Monthly mean values were homogenized, projected onto a grid, and subjected to principle component analysis, which identified two significantly different regions: North and South. Sunshine duration temporal evolution is presented, and possible reasons for differences between the two regions are discussed in the light of a comparison with the trends found in observations of total cloud cover and with results from two neighboring regions: the Alps and Spain. In addition, trends for irradiance records, estimated from sunshine duration records using the Ångström-Prescott formula, are presented too. The major feature of the trends, an increase in sunshine duration from the mid-1980s, was common to both northern and southern Italy; the decrease in the preceding 30 year period was not, as northern Italy had a lower rate of decrease than southern Italy. The few records available during the earliest period of the data set indicate that sunshine duration in Italy increased from the mid-1930s to the mid-1950s. The further steps needed to identify and quantify the mechanisms giving rise to the observed trends and to the reported regional differences in dimming and brightening are outlined.

1. Introduction

Downward solar irradiance at the Earth's surface (global radiation) is the primary energy source for the Earth's climate system. It has a central role in the surface energy balance [e.g., Hartmann *et al.*, 1986; Ohmura and Gilgen, 1993; Wild *et al.*, 2013], driving a large number of processes like diurnal surface and atmospheric boundary layer heating, water evaporation, snow and glacier melting, plant photosynthesis, and related terrestrial carbon uptake [e.g., Wild *et al.*, 2004; Wild, 2009]. Along with the scientific interest, there is also a strong socio-economic benefit in the knowledge of the spatial distribution of global radiation and its temporal trends: it is useful in a wide spectrum of fields such as solar energy production, agriculture, health care, and tourism.

Temporal variations in global radiation depend on many factors, which can be external and internal to the climate system: the most important are cloud cover and atmospheric aerosol [Ramanathan *et al.*, 2001; Stanhill, 2007]. Variations in aerosol concentration can depend on natural causes (e.g., volcanic eruptions), but in many areas there is also a significant contribution related to human activities. Changes in aerosol concentration can also cause variations in cloud cover as the condensation of atmospheric water vapor is influenced by aerosol particles [Lohmann and Feichter, 2005; Rosenfeld *et al.*, 2014].

Temporal variability of global radiation in the last decades is discussed in a large number of papers (see Wild [2009] for a review), with Goldberg and Klein [1971] and Suraqui *et al.* [1974] as two of the pioneering studies. The results suggest a widespread reduction between the 1960s and the early 1980s [e.g., Ohmura and Lang, 1989; Russak, 1990; Stanhill and Moreshet, 1992] and a tendency toward an opposite trend after the 1980s [e.g., Wild *et al.*, 2005]. The first phenomenon is known as “global dimming” [Stanhill and Cohen, 2001], the second as “brightening period” [Wild, 2005]. The causes of this temporal variability are very complex, and they are not completely understood yet. The most relevant drivers of these decadal changes seem to be anthropogenic pollutant emissions [Wild, 2012]. Thus, the recent brightening is associated to air pollution

regulatory actions in developed countries and to declining industrialization in some European countries in the late 1980s [Stanhill, 2005; Streets et al., 2006; Smith and Bond, 2014].

One of the main problems in studying global radiation temporal variability is the small number of sites with reliable long-term records. Extensive networks of pyranometers cover in fact a rather short period [Wild, 2009; Sanchez-Lorenzo et al., 2013a]. It is, therefore, very useful to estimate global radiation temporal variability from other climatic variables (proxy measures) such as total cloud cover (TCC) or daily temperature range (DTR), but probably the most appropriate is sunshine duration (SD) [Stanhill, 2005; Wang et al., 2012].

According to the World Meteorological Organization (WMO), the SD for a given period is defined as the length of time during which direct solar radiation is above 120 W m^{-2} [WMO, 2008]. It has been generally measured with the Campbell-Stokes SD recorder composed of a spherical lens that focuses direct solar radiation onto a paper strip, burning a trace if the irradiance exceeds the instrumental threshold [Sanchez-Lorenzo et al., 2013b]. This threshold ranges from 70 to 280 W/m^2 , depending on a number of factors, the most relevant being the moisture content of the paper strip [WMO, 1969; Sanchez-Romero et al., 2014], although in 1981 the WMO recommended a threshold mean value of 120 W/m^2 [WMO, 2008].

A very important advantage of SD records is that they are available since the late nineteenth century [Sanchez-Lorenzo et al., 2013b], covering a much longer period than global radiation records [Wild, 2009]. Moreover, they are less subjective than TCC observations. Equally, SD is directly correlated to global radiation through Ångström-Prescott formula [Ångström, 1924; Prescott, 1940] (for a review, see Martínez-Lozano et al. [1984]).

Many studies have investigated the temporal behavior of SD for many areas [Wang et al., 2012] including, e.g., the Alpine region [Auer et al., 2007; Brunetti et al., 2009], Western Europe [Sanchez-Lorenzo et al., 2008], Eastern Europe [Brzdil et al., 1994], Switzerland [Ohmura and Lang, 1989; Sanchez-Lorenzo and Wild, 2012], Poland [Matuszko, 2014], Greece [Kitsara et al., 2013], China [Kaiser and Qian, 2002; Liang and Xia, 2005; Xia, 2010; Wang and Yang, 2014; Wang, 2014], the USA [Angell, 1990; Stanhill and Cohen, 2005; Magee et al., 2014], South America [Raichijk, 2012], Iran [Rahimzadeh et al., 2014], India [Soni et al., 2012], Australia [Jones and Henderson-Sellers, 1992], and Japan [Stanhill and Cohen, 2008].

As far as Italy is concerned, papers on the temporal evolution of global radiation or SD in the last decades are not available. The best available information concerns TCC and DTR. Maugeri et al. [2001] studied the temporal evolution of TCC over Italy for the 1951–1996 period by means of 35 synoptic stations. They found a highly significant annual and seasonal negative trend, mainly due to a strong decrease after the 1970s. The stations of the northern part of Italy were then extended and updated to 2005 within the EU FP5 ALP-IMP Project (Multicentennial climate variability in the Alps based on Instrumental data, Model simulations, and Proxy data) and were included in the HISTALP database (Historical Instrumental climatological Surface Time series of the greater Alpine regions) [Auer et al., 2007]: they confirmed the strong decrease since the 1970s [Brunetti et al., 2009].

Brunetti et al. [2006a] studied the temporal evolution of the DTR for the 1865–2003 period by means of 48 Italian secular stations with daily minimum and maximum temperatures. Their results are in good agreement with the global dimming and brightening signals in all seasons but autumn, during which DTR does not increase in the brightening period. It is also worth noting that the Italian DTR records show an increasing trend in the first decades of the twentieth century, which is known as early brightening period [e.g., Ohmura, 2009; Wild, 2009].

In this context, we recently set up a research program aiming at collecting, checking for quality, homogenizing, and analyzing Italian SD records as much as possible. The main steps of this research program and the results of the analyses we performed are presented in this paper. After the introduction, section 2 describes the data sources and section 3 discusses quality control, homogenization, gap filling, gridding, and clustering into homogenous regions. In section 4, the average regional records are subjected to trend analysis and compared with records of other areas and with Italian TCC records. Finally, in section 5, some conclusive remarks are outlined.

2. Data

The SD records used in this paper were obtained from three main data sources: (a) the paper archive of the former Italian Central Office for Meteorology (24 records), which is managed by CRA-CMA, a research unit of

the National Agricultural Research Council (Consiglio per la Ricerca e la Sperimentazione in Agricoltura), (b) the database of Italian Air Force synoptic stations (AM—Aeronautica Militare) (47 records), and (c) the National Agrometeorological database (BDAN—Banca Dati Agrometeorologica Nazionale) (59 records), which is also managed by CRA-CMA. In addition, we considered four records (Pontremoli, Varese, Modena, and Trieste) from university and local observatories.

Specifically, CRA-CMA hosts the archive of the former Italian Central Office for Meteorology. The digitalization of this archive is in progress even though up to now less than 30% of the available data have been transferred to computer readable form [Beltrano *et al.*, 2012a, 2012b] and included in the BDAN. We digitalized daily SD data from 24 observatories.

The Italian Air Force records were already available in digital form. A brief summary on the history of these observations is recorded in a report of the *Italian Air Force* [2012], which shows also some statistics on data availability, highlighting a much better situation for SD with respect to solar radiation.

BDAN includes records from automatic stations and from the CRA-CMA traditional network (only 25 stations of this network are still in operation). The automatic stations are from AM network, from Italian agency for civil aviation (ENAV—Ente Nazionale Assistenza al Volo) network, and from the National Agrometeorological network (RAN—Rete Agrometeorologica Nazionale).

Pontremoli and Varese records were collected, respectively, at “Osservatorio Meteorologico Marsili” and at “Centro Geofisico Prealpino.” The former observatory is managed by the Italian Society for Meteorology [Ratti, 2010], the latter is managed by a local meteorological association. Modena and Trieste records were collected, respectively, since 1893 at “Osservatorio Geofisico” of Modena University [Lombroso and Quattrocchi, 2008] and since 1886 at different sites all located within 1.6 km in the city of Trieste [Stravisi, 2004]. We consider here only the data since 1936 as the focus of this paper is on the entire Italian territory, and before 1936 there are only these two series.

For some sites, we set up composite records, merging data of the same station from different sources. Moreover, for some records we merged data from different sites. They concern stations at short distances and belonging to areas with homogeneous geographical features. Additional information on the SD records is shown in Table 1 that lists the records by data sources, providing station names, coordinates, and elevations. The table also provides information on the SD recorders, on the years supplying data, and on composite and merged records.

The final data set encompasses 104 SD daily records covering the entire Italian territory for the 1936–2013 period. The spatial distribution of the stations (Figure 1) is uniform, with the only exception of the Alps and Apennines. So, most of the stations are located in the Italian plains or coastal areas. Data availability versus time is rather inhomogeneous (Figure 2). The best data coverage concerns 1958–1964, 1971–1977, and 1982–2013, while the period with the most critical situation corresponds to the first 22 years (1936–1957).

3. Data Preprocessing

3.1. Quality Check and Calculation of Monthly Values

All daily records were checked in order to find out and correct gross errors [Aguilar *et al.*, 2003]. Moreover, station coordinates were checked matching the consistency of the coordinates with the information from station metadata and controlling elevation in relation to position.

All records were expressed in hours and tenths of hour. Monthly records were calculated when the fraction of missing data did not exceed 10%. They were then converted into relative SD records that express the ratio between measured and maximum possible SD.

3.2. Data Homogenization

Climatic records are often affected by nonclimatic signals which have to be identified and eliminated [Aguilar *et al.*, 2003]. They can be caused by changes in the condition or in the management of the corresponding meteorological station and by changes in the area surrounding the station [Brunetti *et al.*, 2006a]. As far as Italian sunshine duration data are concerned, a major issue is linked to the different instrumentation used to measure sunshine duration in the different networks (see Table 1).

Table 1. Details on the Records in the SD Data Set

Network/Data Source	Region	Station	Latitude (deg)	Longitude (deg)	Elevation (m)	Period	Composite Record	Instrument	
AM	N	Alghero	40.633	8.283	23	1958–1989	No	Campbell-Stokes sunshine duration recorder	
		Bologna Borgo Panigale	44.530	11.300	36	1958–1991	No		
		Bolzano	46.467	11.333	241	1958–1990	No		
		Capo Caccia	40.560	8.164	202	1990–2004	No		
		Cervia	44.217	12.300	10	1989–2013	Yes		
		Elba	42.733	10.400	397	1984–2004	No		
		Genova Sestri	44.413	8.868	2	1962–1989	No		
		Milano Linate	45.450	9.270	107	1958–2000	No		
		Monte Cimone	44.194	10.700	2165	1958–2004	No		
		Monte Terminillo	42.451	12.983	1874	1958–2004	No		
		Paganella	46.143	11.037	2125	1990–2004	No		
		Pisa San Giusto	43.680	10.380	7	1958–2004	Yes		
		Plateau Rosa	45.933	7.700	3488	1958–1999	No		
		Ponza	40.917	12.950	185	1991–2004	No		
		Torino Bric della Croce	45.030	7.730	710	1982–2004	No		
		Torino Caselle	45.187	7.646	301	1958–1993	No		
		Udine Rivolto	45.967	13.033	53	1982–2004	No		
		Venezia Tessera	45.500	12.330	2	1961–1989	No		
		Vigna di Valle	42.080	12.220	262	1982–2013	Yes		
		Viterbo	42.433	12.050	308	1992–2004	No		
		S	Campobasso	41.570	14.650	793	1973–2004		No
			Crotone	38.996	17.080	155	1958–1997		No
			Monte Scuro	39.333	16.400	1710	1993–2004		No
			Napoli Capodichino	40.850	14.300	88	1958–1997		No
			Pantelleria	36.817	11.967	191	1958–2004		No
			Pescara	42.430	14.200	10	1958–1990		No
			Ustica	38.700	13.183	250	1958–2004		No
AM—updated by BDAN (ENAV and AM networks)	N		Capo Mele	43.954	8.169	220	1963–2013	No	Campbell-Stokes sunshine duration recorder - SIAP-Micros transducer
			Piacenza	44.917	9.733	138	1991–2008	No	
			Roma Ciampino	41.800	12.583	129	1958–2009	No	
		Treviso Sant'Angelo	45.650	12.183	18	1988–2008	No		
		Trieste	45.650	13.783	8	1958–2013	No		
		Verona Villafranca	45.383	10.867	68	1991–2009	No		
		S	Brindisi	40.650	17.950	15	1958–2013	No	
			Capo Bellavista	39.934	9.710	138	1992–2013	No	
			Capo Palinuro	40.024	15.275	184	1958–2013	No	
			Cozzo Spadaro	36.686	15.132	46	1992–2013	No	
			Foggia Amendola	41.533	15.717	60	1959–2009	No	
			Gela	37.076	14.225	11	1971–2013	No	
			Grazzanise	41.050	14.067	9	1992–2013	Yes	
			Messina	38.201	15.553	59	1960–2013	No	
			Santa Maria di Leuca	39.817	18.350	104	1993–2013	No	
			Termoli	42.004	14.996	44	1991–2013	No	
		Trapani Birgi	37.917	12.500	7	1961–2009	No		
RAN/BDAN	N	Cagliari Elmas	39.250	9.050	4	1958–2006	No	SIAP-Micros transducer threshold: 120 W/m ² , range: 0 ÷ 1500 W/m ² , spectrum: 0.2±1.1 μm, accuracy: 2.4 W/m ² , 300°continuous scan	
		Borgo San Michele	41.450	12.900	12	1995–2013	No		
		Caprarola	42.327	12.177	650	1994–2013	No		
		Carpeneto	44.683	8.624	230	1994–2013	No		
		Cividale	46.091	13.419	130	1997–2013	No		
		Chilivani	40.617	8.936	216	1994–2013	No		
		Fiume Veneto	45.921	12.724	19	1996–2013	No		
		Marsciano	43.005	12.303	229	1991–2013	Yes		
		Montanaso Lombardo	45.332	9.457	83	1994–2013	No		
		Piubega	45.226	10.533	40	1994–2013	Yes		
		San Casciano	43.671	11.152	230	1994–2013	No		
		San Piero a Grado	43.669	10.348	3	1994–2013	No		
		Santa Fista	43.523	12.129	311	1994–2013	No		
		Susegana	45.852	12.259	67	1994–2013	No		
		Verzuolo	44.598	7.484	420	1995–2013	No		
		Vigalzano	46.068	11.234	539	1999–2013	No		

Table 1. (continued)

Network/Data Source	Region	Station	Latitude (deg)	Longitude (deg)	Elevation (m)	Period	Composite Record	Instrument
CRA-CMA	S	Aliano	40.283	16.315	250	1998–2013	No	Campbell-Stokes SD recorder
		Campochiaro	41.475	14.538	502	1994–2013	No	
		Castel di Sangro	41.750	14.098	810	1998–2013	No	
		Libertinia	37.543	14.583	183	1994–2013	No	
		Matera	40.654	16.613	370	1999–2013	Yes	
		Monsampolo	42.888	13.797	43	1994–2013	No	
		Palo del Colle	41.054	16.633	191	1994–2013	No	
		Piano Cappelle	41.114	14.828	152	1994–2013	Yes	
		Pietranera	37.506	13.517	158	1994–2013	No	
		Pontecagnano	40.620	14.921	29	1997–2013	No	
		Santa Lucia	39.978	8.619	14	1994–2013	No	
		Santo Pietro	37.119	14.525	313	1994–2013	No	
	Sibari	39.739	16.450	10	1994–2013	No		
	Turi	40.921	17.011	230	1994–2013	No		
	N	Alasio	44.000	8.170	32	1937–2013	Yes	
		Chiavari	44.315	9.323	25	1937–2001	No	
		Civitavecchia	42.083	11.783	23	1969–1992	No	
		Cuneo	44.400	7.533	536	1961–1993	No	
		Faenza	44.287	11.879	55	1949–1992	No	
		Imperia	43.877	8.016	54	1952–2011	No	
		Milano Brera	45.472	9.188	147	1948–1971	No	
		Parma	44.804	10.315	53	1936–2008	No	
		Pavia	45.183	9.129	82	1936–1974	No	
		Pesaro	43.902	12.883	14	1937–2007	No	
		Piacenza Collegio Alberoni	45.035	9.726	72	1941–1998	No	
		Pisa	43.679	10.320	2	1957–1989	Yes	
		Roma Collegio Romano	41.898	12.481	57	1942–2013	No	
		Salo	45.608	10.522	110	1946–2013	No	
		Savona	44.307	8.457	24	1946–2011	No	
		Urbino	43.725	12.653	476	1943–1999	No	
		Verbania Pallanza	45.917	8.550	241	1975–1991	No	
		Voghera	44.983	8.967	108	1974–1984	No	
		Terni	42.567	12.650	170	1961–2000	No	
S		Acireale Agrumicoltura	37.620	15.152	208	1971–1984	Yes	
		Catania	37.504	15.079	65	1940–1977	No	
	Foggia Podere	41.500	15.563	90	1950–1962	No		
	Foggia Quindicina	41.550	15.519	50	1951–1962	No		
	Gaeta	41.220	13.567	50	1939–1998	No		
	Lucugnano	39.948	18.292	130	1938–1969	No		
	Taranto	40.467	17.254	22	1937–2013	No		
	Modena	44.648	10.930	76	1936–1984	No		
	Pontremoli	44.377	9.877	257	1994–2013	No		
	Trieste Hortis	45.648	13.766	35	1936–2010	No		
University and local observatory	N	Varese	45.834	8.820	427	1983–2013	No	Campbell-Stokes SD recorder and LSI-Lastem SD recorder threshold: 120 W/m ² , range: 0 ÷ 1500 W/m ² , spectrum: 300 ÷ 110 nm, accuracy: 5 W/m ²

We subjected, therefore, all our monthly records to a homogenization procedure based on a relative homogeneity test as described by *Brunetti et al.* [2006a]. In this procedure, each series is tested against 10 other series by means of the Craddock test [Craddock, 1979]. When a break is identified in the test series, some reference series are chosen among those that prove to be homogeneous in a sufficiently large period centered on the break and that correlate well with the test series. Several series are used in order to better identify the break and to get adjustments that are more reliable. When a break is identified, the preceding portion of the series is corrected, leaving the most recent portion unchanged. This allows updating the records without considering adjustment factors.

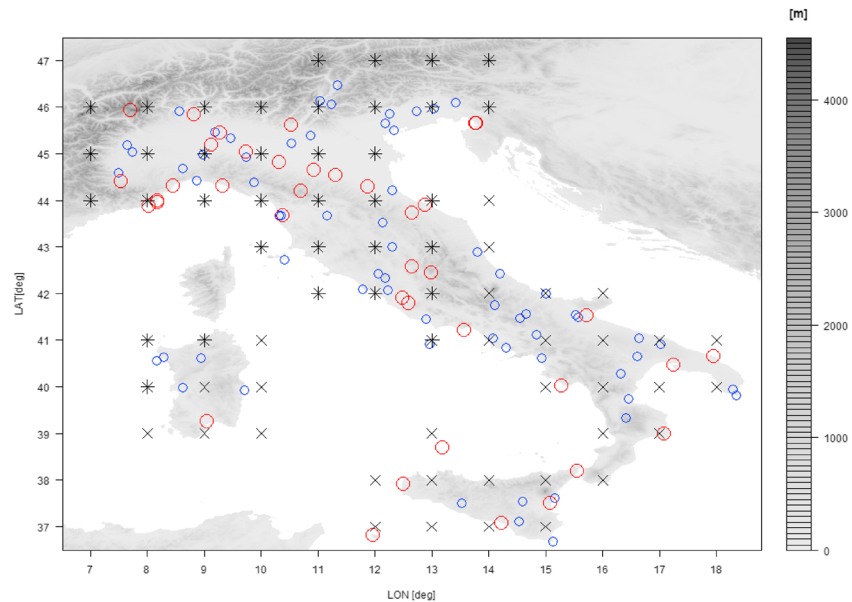


Figure 1. Spatial distribution of the stations and points of the grid-mode version of the data set (see section 3.5): stars and crosses represent, respectively, northern and southern Italy grid points. The figure also shows the orography of the region and gives evidence of the length of the station records, with big red circles indicating stations with more than 30 years of data.

The ability of the procedure to detect breaks depends on the spatial coherence of the data and on the density of the record network. Some information on such issues is given in Figure 3. It shows that the common variance between two stations falls to about 50% at a distance of 150 km and that it is extremely difficult to apply the homogenization procedure before 1946. In this period, in fact, there is a very low number of records within a radius of 150 km from each station with available data.

After homogenization, only 34 out of 104 records resulted homogeneous, whereas the remaining 70 were homogenized. A total number of 116 breaks were found. By plotting the number of detected breaks versus time, we found a significant increase (Figure 4a); this is an expected result as the probability of breaks is indeed linked to data availability (Figure 2). However, there is an increase in the number of detected breaks even when we normalize them with respect to the number of available series per year (Figure 4b), due to the very low number of breaks before 1950. This is related to the higher performances of all relative homogeneity tests with the increase of station density.

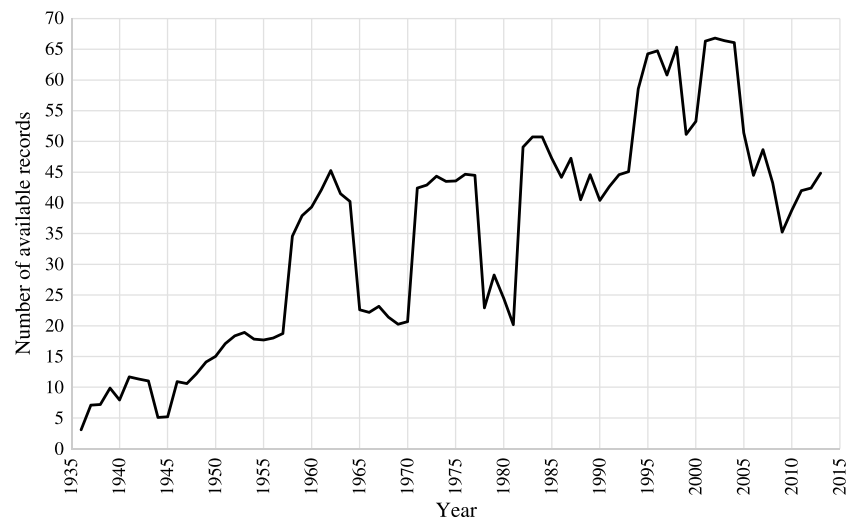


Figure 2. Temporal evolution of the number of available records.

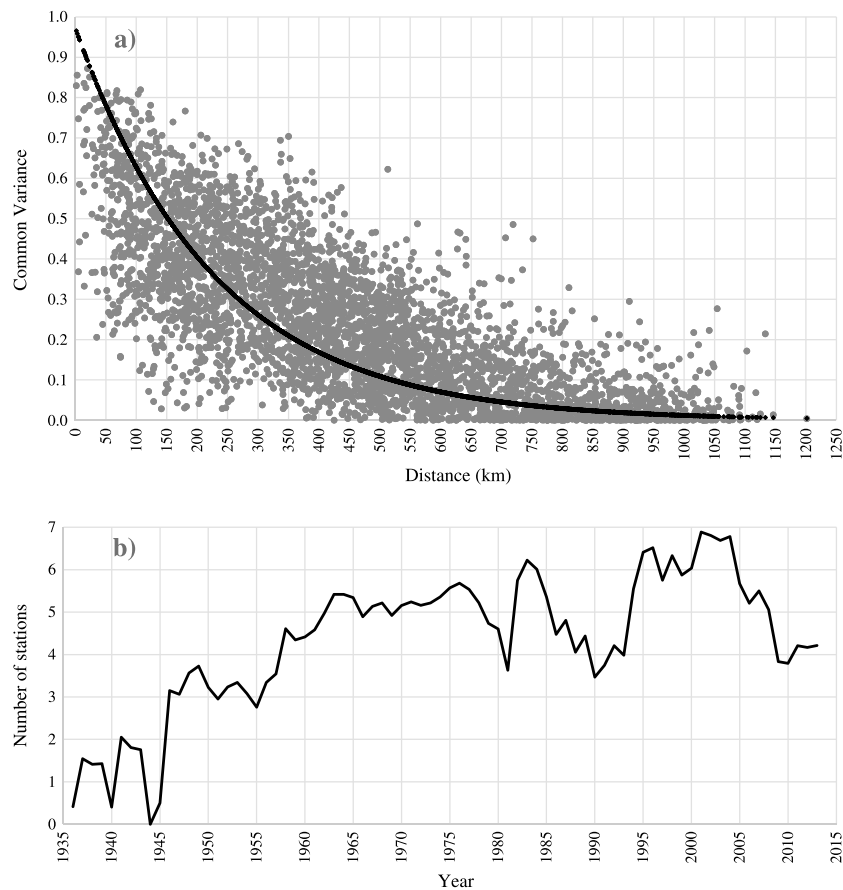


Figure 3. (a) Common variance versus distance of monthly sunshine duration records. In order to remove the effect of the annual cycle, common variance has been calculated after deseasonalization of the records; (b) temporal evolution of the average number of available stations within a radius of 150 km from each station with available data.

In order to better understand the effect of the homogenization procedure, we analyzed the adjustment series obtained performing the ratio between the homogenized and the original series. Figure 5 shows the curve obtained by averaging the mean annual adjustments overall single records, together with their absolute range. The large absolute range underlines how homogenization is important to get reasonable single station series. This is particularly evident for some records of the archive of the former Italian Central Office for Meteorology (i.e., Cagliari, Cuneo, and Taranto), with adjustments up to 1.5. Even though the adjustments cover a wide range of values, their average is rather close to one, especially since 1980. In the 1961–1979 period, the average adjustments (from 1.02 to 1.06) are higher than 1.0, this means that the original data were systematically increased to get homogenous data; however, it is due only to a few records with rather large adjustments. In the years before the 1960s (adjustments from 0.96 to 1), there is a tendency to have smaller values in the homogenized records with respect to the original ones. The necessity of reducing SD before 1960 to get homogeneous series may be due to the strong urbanization which occurred in Italy in the following decades, causing a reduction in the sky-view factor for some urban observatories of the CRA-CMA network and producing relatively lower SD in the following years.

3.3. Gap Filling and Calculation of Monthly Anomaly Records

After homogenization, we filled the gaps in each monthly record. The record to be used as reference for the estimation of a missing datum was selected among those fulfilling two conditions: distance within 500 km from the record under analysis and availability of at least 10 monthly values in common with it in the month of the gap. If no records fulfilled these conditions, the missing datum was not estimated. The records fulfilling these conditions were ranked considering the product of a distance and an elevation factor. These factors were defined as in Brunetti *et al.* [2013], using Gaussian weights. For distance, the

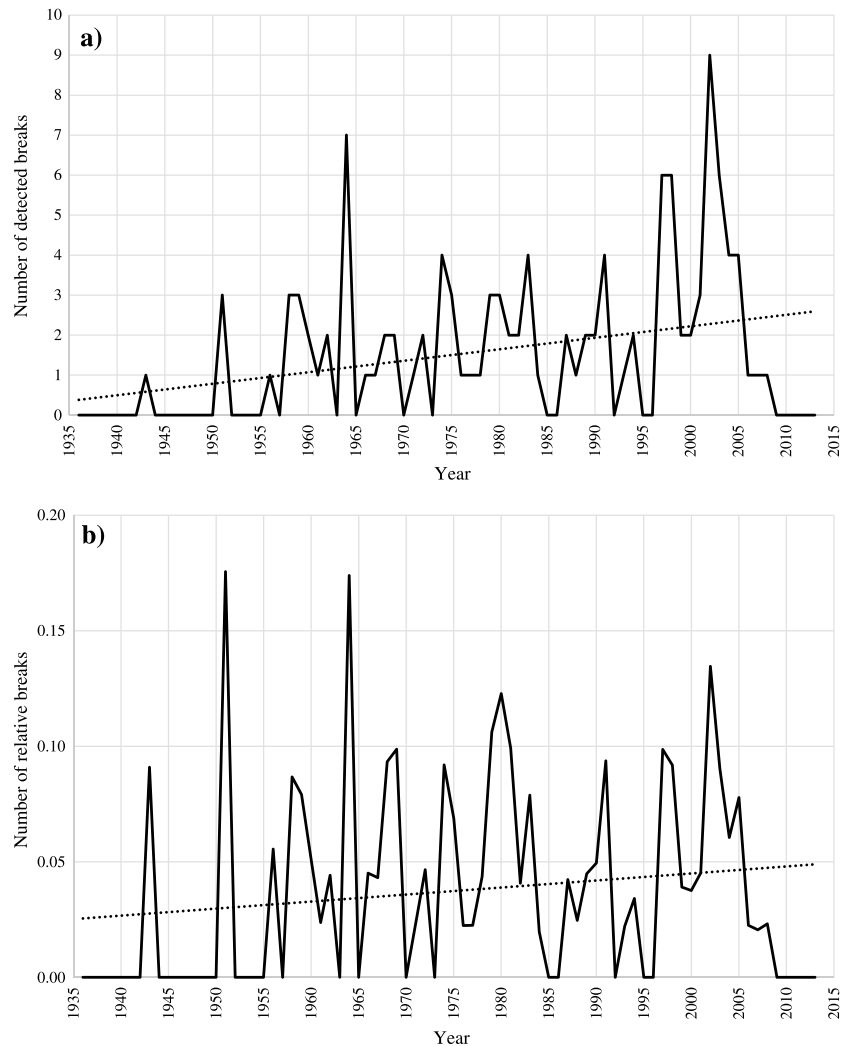


Figure 4. (a) Number of detected breaks per year in the sunshine duration data set and (b) number of detected breaks normalized by the number of available series. The regression lines are shown (dotted lines) too.

weight decreases to 0.5 at 300 km. For elevation difference, if station elevation is under 500 m, it decreases to 0.5 at 250, whereas for higher stations, it decreases to 0.5 at half of station elevation. The record with the highest rank was then selected as reference record, and the gap was filled under the assumption of the constancy of the ratio between incomplete and reference series. The procedure has been checked with a leave-one-out approach, considering each available value of each record as missing and estimating it: about 50% of the ratios between the original values and the estimated ones resulted between 0.95 and 1.05; about 90% of them resulted between 0.85 and 1.15.

After gap filling, we considered only the 95 records for which at least 90% of the data were available in the 1984–2013 period and transformed them into anomaly records, with respect to the monthly 1984–2013 normals. Besides monthly anomaly records, also seasonal and annual anomaly records were produced. Seasons are defined according to the scheme December-January-February, March-April-May, June-July-August, and September-October-November, and winter is dated according to the year in which January and February fall. Years are defined by the December–November period. For the first year, the winter season is calculated only with January and February, while the year is calculated only with the January–November period.

3.4. Gridding

Starting from the 95 gap-filled anomaly series, we generated a gridded version of the monthly, seasonal, and annual SD anomalies. The aim was to balance the contribution of areas with a higher number of stations with

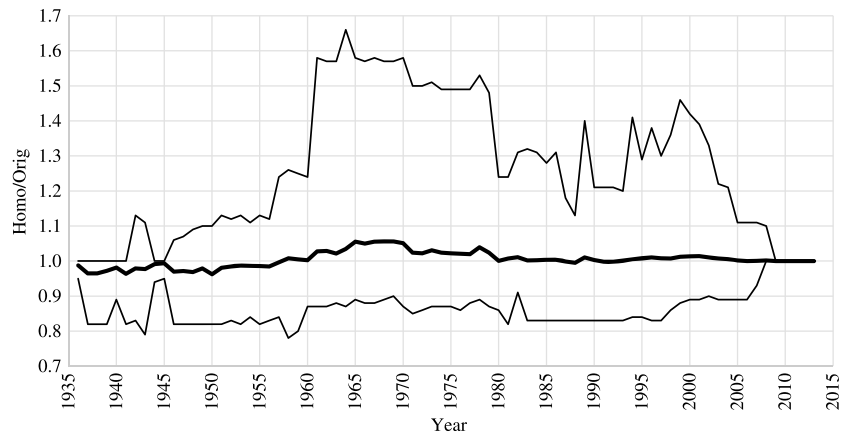


Figure 5. Mean annual adjustment series obtained by calculating the annual average adjustment overall series (bold line). The figure shows the maximum range in the adjustments too.

those that have a lower station coverage. We used a grid of $1^\circ \times 1^\circ$ following the technique described by Brunetti et al. [2006a] and Sanchez-Lorenzo et al. [2007], which is based on an Inverse Distance Weighting approach with the addition of an angular term to take into account the anisotropy in spatial distribution of stations.

Distance weights (w_i^d) were calculated as for the gap-filling procedure, with a decrease to 0.5 for distance equal to $\bar{d}/2$ from the grid point under analysis. Here \bar{d} is defined as the mean distance from one grid point to the next one calculated overall adjacent points of the grid: it turns out to be about 130 km. The angular term (α_i) is that used by New et al. [2000]. The station weights were then obtained as in New et al. [2000] by means of $w_i = w_i^d(1 + \alpha_i)$. Gridded values were calculated only when either a minimum of two stations at a distance smaller than \bar{d} were available or a minimum of one station at a distance smaller than $\bar{d}/2$. Grid values were calculated by considering all stations within a distance of \bar{d} .

The grid spans from 7 to 19°E and from 37 to 47°N, with 68 points over the Italian territory (Figure 1).

3.5. PCA and Regional Average Records for Italian Main Climatic Regions

Monthly anomaly records were subjected to principal component analysis (PCA) in order to identify areas with similar SD temporal variability. This technique allows the identification of a small number of variables, known as principal components, which are linear functions of the original data and which maximize their explained variance [Preisendorfer, 1988; Wilks, 1995]. The analysis focused on the 1958–2013 period because here we had more available data.

We applied PCA both to station and grid point records. As the results are very similar, we discuss only the grid point results. Table 2 shows the eigenvalues, the explained variances, and the cumulative explained variances of the first six eigenvectors, which are those with eigenvalues greater than 1. They explain more than 89% of the total variance of the data set.

Table 2. PCA of the Gridded Data Set ^a

EOF	Nonrotated			Varimax Rotated		
	Eigenvalues	Variance (%)	Total Variance (%)	Eigenvalues	Variance (%)	Total Variance (%)
1	40.3	59.3	59.3	29.1	42.3	42.3
2	11.9	17.6	76.9	23.2	34.1	76.9
3	3	4.5	81.4			
4	2.7	3.9	85.3			
5	1.6	2.3	87.6			
6	1.1	1.6	89.2			

^aEigenvalues, explained variances, and cumulative explained variances of nonrotated and rotated EOFs obtained from the PCA applied to the gridded data set.

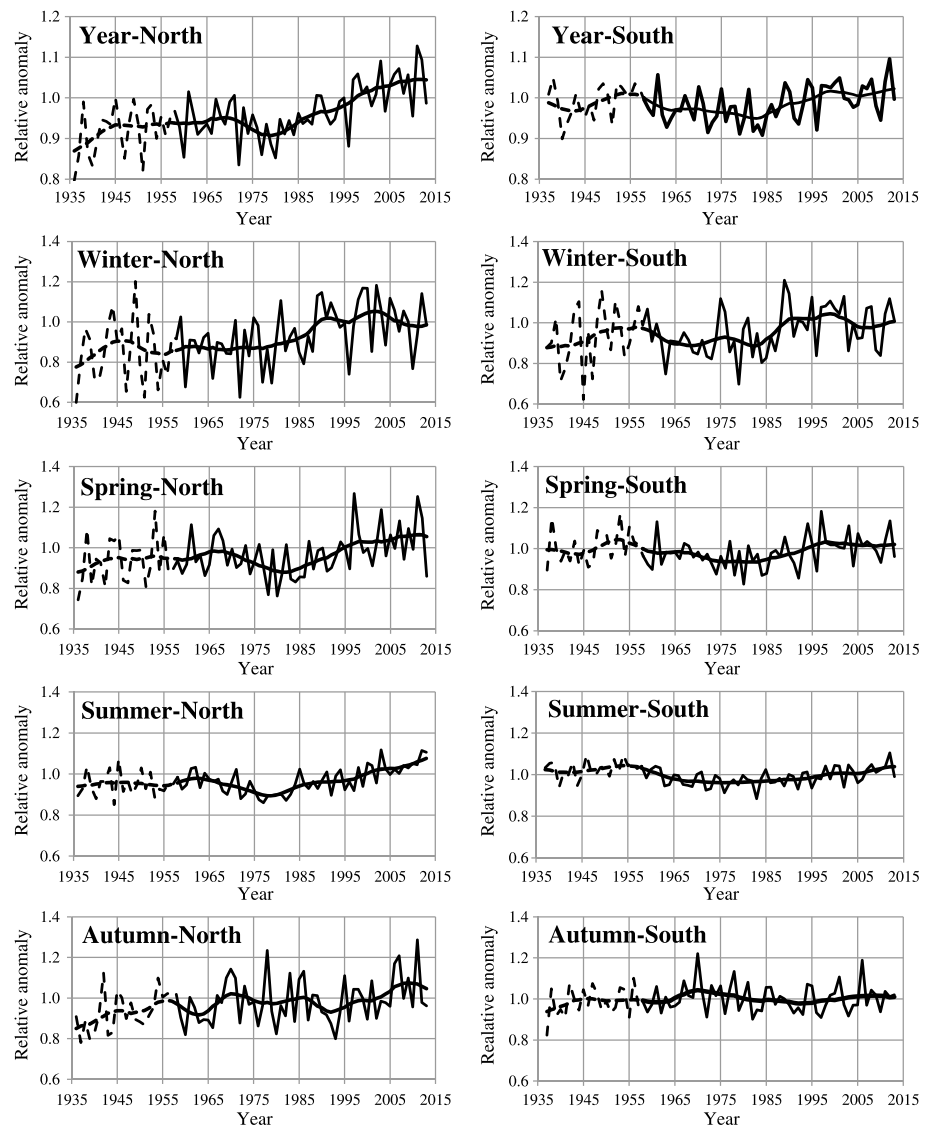


Figure 6. Average annual and seasonal (left column) northern and (right column) southern Italy sunshine duration series (thin lines), plotted together with an 11 year window-3 year standard deviation Gaussian low-pass filter (thick lines). The series are expressed as relative deviations from the 1984–2013 means. Dashed lines are used prior to 1958 owing to the lower number of records for the initial period. Annual graphs are expressed with an expanded scale with respect to seasonal ones.

To obtain more physically meaningful patterns we selected to rotate, by means of a VARIMAX rotation [Von Storch, 1995], the first two empirical orthogonal functions (EOFs), which are those that account for more than 5% of the original variance of the data set. The loading patterns (figure not shown) allowed to identify two regions are the following: northern Italy (36 grid points) and southern Italy (32 grid points) (Figure 1). Finally, we calculated the regional monthly, seasonal, and annual mean series from the gridded data set simply by averaging all corresponding grid point anomaly records.

4. Results and Discussion

4.1. Trend Analysis of the Seasonal and Annual Regional Records

The average northern and southern Italy seasonal and annual SD records are shown in Figure 6, together with a low-pass filter working on 11 year windows that considers Gaussian weights decreasing to e^{-1} at 3 years from the center of the window.

These curves indicate an increase starting from the 1980s. This signal concerns both northern and southern Italy and all seasons, with the only exception of autumn that shows an increasing tendency only in northern Italy starting from about 1995. Before this brightening signal, there is a decreasing tendency: it is, however, less evident than the more recent increase. In northern Italy, it concerns spring and summer and the period from about middle of the 1960s to the beginning of the 1980s; in southern Italy, it concerns also winter and seems to start from about the end of the 1950s. In the early period, from the 1930s to the 1950s, there is some evidence of an increasing tendency. This early brightening signal concerns, however, a period in which data availability is low, causing a greater uncertainty in the regional records. Moreover, it is rather weak and different for northern and southern Italy, both in terms of seasons and corresponding periods taken into account.

In order to better investigate the increasing and decreasing tendencies highlighted in Figure 6, we subjected the records to running trend analysis [Brunetti *et al.*, 2006b]. Specifically, we estimated slopes by applying linear least squares regression to all subintervals of at least 20 years of the 1936–2013 period. The results are shown in Figure 7, where window widths and the starting years of the windows that the trends refer to are represented on y and x axes, respectively. Slopes are represented by the colors of the corresponding pixels. Pixels are plotted only for trends with a significance level of 0.1. Significances are evaluated by the Mann-Kendall nonparametric test [Sneyers, 1992]. This type of running trend analysis is an instrument to investigate trends in depth and to produce plots that show trends on a wide range of time scales.

First, in Figure 7, it underlines the evident brightening of the last decades of the study period: it is significant in all cases, with increases up to near 10%/decade, with the only exception of autumn in southern Italy. The highest increase concerns the decades starting at the beginning of the 1980s. Second, it shows that also the dimming signals highlighted in Figure 6 are significant. In northern Italy, they concern only spring and summer for the subperiods ending in the 1980s, whereas in southern Italy there is a dimming period also in winter and at annual scale. Thus, in this region the dimming period is more evident and slightly anticipated with respect to northern Italy. Third, it shows that the early brightening signal is significant only in autumn in northern Italy. This latter signal, even though not significant at a seasonal level, is significant in some cases for the annual record both for northern and southern Italy.

Figure 7 (left column) highlights that in northern Italy the brightening of the last decades is both stronger and longer than the previous dimming. In fact, also in the seasons that show a significant dimming in the 1960s and 1970s, the trend over the widest windows is significantly positive: for the 1936–2013 period, it ranges from $1.1 \pm 0.3\%$ /decade in summer to $2.8 \pm 0.7\%$ /decade in autumn. On the contrary, Figure 7 (right column) gives evidence that in southern Italy the dimming and the following brightening are comparable in slope and length, with the only exception of autumn where these signals are not present. Therefore, the trend of the widest windows is generally not significant. In this region, there is a significant positive long-term trend only for the winter record ($1.5 \pm 0.6\%$ /decade over the 1936–2013 period) and for a few windows for the annual record, whereas in summer there are some rather wide windows with negative trends.

In order to get a first estimation of global radiation trends, we estimated global irradiance data from the corresponding SD records by means of Ångström-PreScott formula [Ångström, 1924; Prescott, 1940]. Specifically, we used the coefficients reported by Spinoni *et al.* [2012], which give a preliminary estimation of this formula for Italy. The resulting records were then transformed into anomalies with respect to the monthly averages of the 1984–2013 period and were used to get northern and southern Italy global radiation (expressed as mean irradiance, in W m^{-2}) anomaly records. The trends of these records are presented in Table 3 for five periods, i.e., the entire period covered by the data, the period with best data availability, and three intervals (1951–1980, 1981–2000, and 1981–2013), which can be useful for comparison with other studies. The results for the annual records give evidence of a decrease in the global dimming period (1951–1980), which is not significant in northern Italy and is slightly above 3 W m^{-2} per decade in southern Italy. Southern Italy trend is in line with trends reported in other worldwide areas [Stanhill and Cohen, 2001; Liepert, 2002; Wild, 2009, 2012] and Europe [Norris and Wild, 2007; Chiacchio and Wild, 2010; Sanchez-Lorenzo *et al.*, 2013c]. The increase in the following period is significantly stronger in northern Italy (over 5 W m^{-2} per decade), whereas it is comparable to the previous decrease in southern Italy. Also in this period, at an annual scale, southern Italy results are in good agreement with reported trends in Europe [Wild, 2009, 2012; Sanchez-Lorenzo *et al.*, 2013a, 2013b]. Nevertheless, northern Italy trends exhibit a tendency toward higher increase as compared to most of the sites in Europe, even in

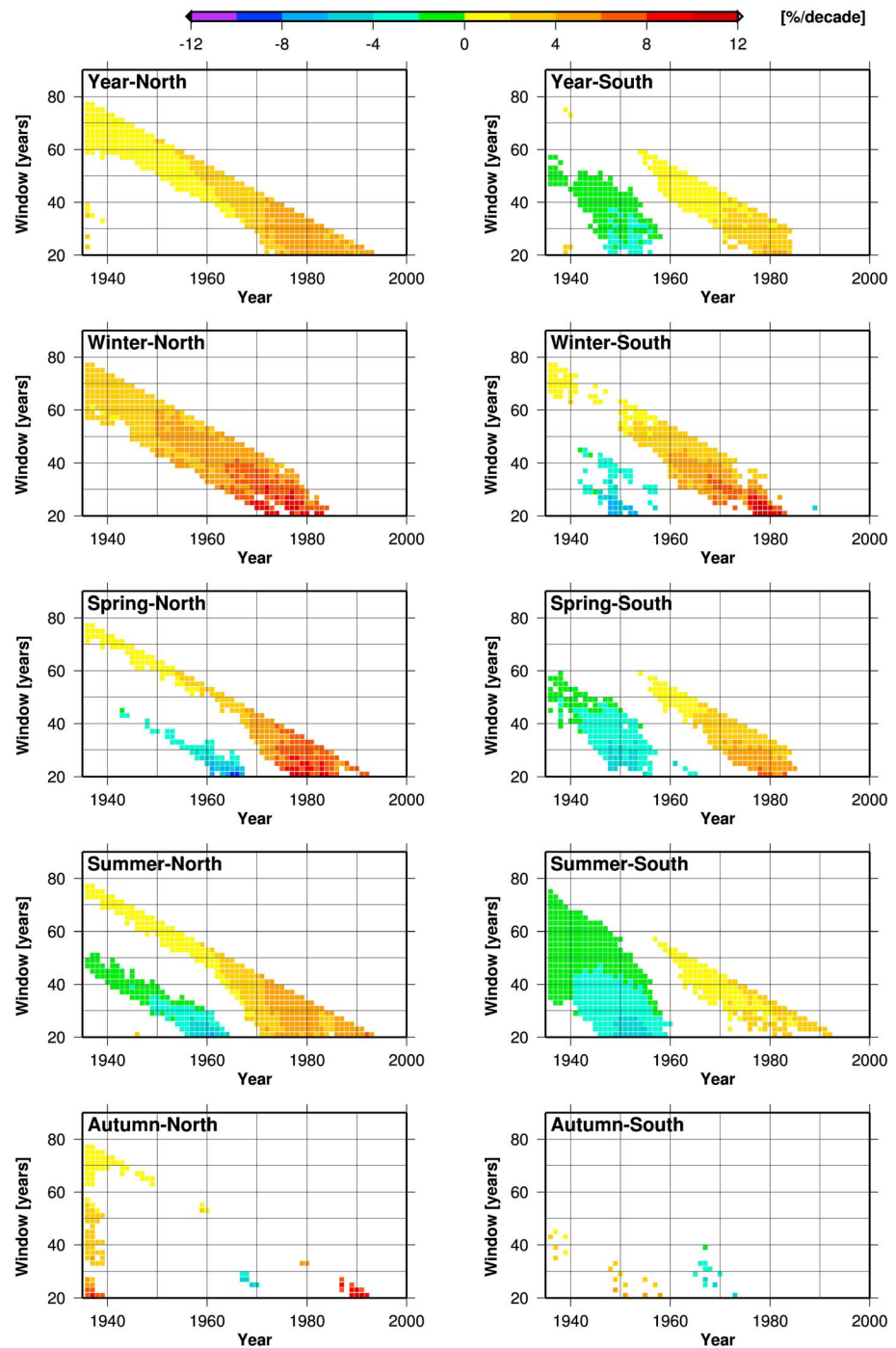


Figure 7. Running trend analysis for the (left column) northern Italy and (right column) southern Italy annual and seasonal records. The y axis represents window width, and the x axis represents starting year of the window over which the trend is calculated. Only trends with significance level of at least 0.1 are plotted.

Central Europe [Ruckstuhl et al., 2008; Philipona et al., 2009; Sanchez-Lorenzo and Wild, 2012], although a trend of around 5 W m^{-2} is also reported in Germany during the period 1985–2005 [Wild et al., 2009] and the region of the Po Valley and Central Europe over the period 1980–2012 [Nabat et al., 2014].

4.2. Comparison With Sunshine Duration Records of Other Areas

SD is one of the variables considered by the HISTALP Project that aimed at setting up a wide data set of instrumental time series for the Greater Alpine Region (GAR, 4–19°E, 43–49°N) [Auer et al., 2007]. This data set

Table 3. Global Radiation Trends ^a

		Annual	Winter	Spring	Summer	Autumn
North	1936–2013	1.5 ± 0.3	1.3 ± 0.3	1.8 ± 0.6	1.7 ± 0.5	1.1 ± 0.3
	1958–2013	2.1 ± 0.4	1.8 ± 0.5	2.5 ± 1.0	3.3 ± 0.8	1.0 ± 0.6
	1951–1980	–	+	–	–3.4 ± 1.6	+
	1981–2000	5.7 ± 1.3	5.3 ± 2.2	10.6 ± 4.1	7.4 ± 3.1	–
	1981–2013	5.1 ± 0.8	+	7.7 ± 2.2	8.9 ± 1.4	2.4 ± 1.3
South	1936–2013	+	0.8 ± 0.4	+	–	+
	1958–2013	1.2 ± 0.4	1.4 ± 0.5	1.8 ± 0.8	1.6 ± 0.7	–
	1951–1980	–3.1 ± 0.9	–2.0 ± 1.3	–6.2 ± 1.9	–7.0 ± 1.6	+
	1981–2000	5.1 ± 1.7	7.0 ± 2.5	+	5.7 ± 2.9	–
	1981–2013	3.0 ± 0.8	+	3.9 ± 1.8	5.1 ± 1.4	+

^aValues are expressed in W/m² per decade. Values are shown only for significance greater than 90%, whereas bold characters indicate significance greater than 95%. For not significant trends, only the sign of the slope is given.

has been analyzed by *Brunetti et al.* [2009] in a paper discussing and comparing long-term changes and high-frequency variability of these variables: they studied four regions representing different GAR low-level areas (northwest, northeast, southwest, and southeast) and an additional mean series for high-level locations. The southwest and southeast records concern a wide area covering also the northern part of Italy. When the HISTALP data set had been set up, no long-term SD records were available for Italy. Therefore, the HISTALP southwest and southeast SD records were constructed without considering Italian series. Thus, it is very interesting to compare northern Italy SD records with the corresponding HISTALP southwest and southeast records, which are here combined in an average record representative of the southern part of the GAR.

This comparison is shown in Figure 8 (left column) for the annual and seasonal low-pass filter records for the period of best common data availability (1958–2007). Figure 8 shows good agreement between HISTALP records and those considered in this paper, as for both data sets the recent brightening signal is clearer than the previous dimming signal. It is worth noting that the Italian and the HISTALP SD records have been set up using completely independent data and homogenization procedures. Therefore, the good agreement between these records is not only interesting, as it shows that long-term SD exhibits a rather coherent signal over a large region such as the southern part of the GAR, but it is also useful to increase our confidence in the quality of the regional SD records both for HISTALP and Italian data sets. This point is very important also to shed light on some apparent inconsistencies between the HISTALP SD and TCC records detected by *Brunetti et al.* [2009]: the authors highlighted a disagreement between the long-term tendencies of the two variables, suggesting that some biases could affect one of these variables or both of them. The agreement between HISTALP SD records and our new SD data set suggests that the inconsistencies between the HISTALP SD and TCC records are possibly due to problems in the HISTALP TCC records.

The behavior of northern Italy and GAR southern regions is indeed rather peculiar, as most publications do not report a significant increase either for SD or for global radiation in the 1958–2007 period. Thus, the SD records of this area could support the hypothesis of *Wang et al.* [2013] that suggests that the dimming period in global radiation records could have been overestimated, due to some instrumental problems. More specifically, *Wang et al.* [2013] compared global radiation records measured by single pyranometers with those obtained by summing diffuse and direct components, which are measured by shaded pyranometers and pyrhemometers, respectively. They conclude that there are statistically significant differences between both methods to estimate global radiation, and state that the trend rates during the dimming period, when only single pyranometers were available, would have been lower if measured using global radiation from shaded pyranometer and pyrhemometer data. Further research is needed on this issue; in this paper, based on comparison with TCC records (see section 4.3), we suggest, however, that the behavior of northern Italy SD is linked to a peculiar evolution of TCC.

As far as southern Italy is concerned, we perform the comparison with a more Mediterranean-like area, such as Spain. We show, therefore, in Figure 8 (right column) southern Italy annual and seasonal low-pass filter records together with corresponding records from *Sanchez-Lorenzo et al.* [2007] for the period 1961–2004. Specifically, we consider the eastern Spain records shown in the first column of Figure 7 of that paper. The results indicate that in southern Italy the dimming in the 1960s and 1970s is indeed weaker than in Spain.

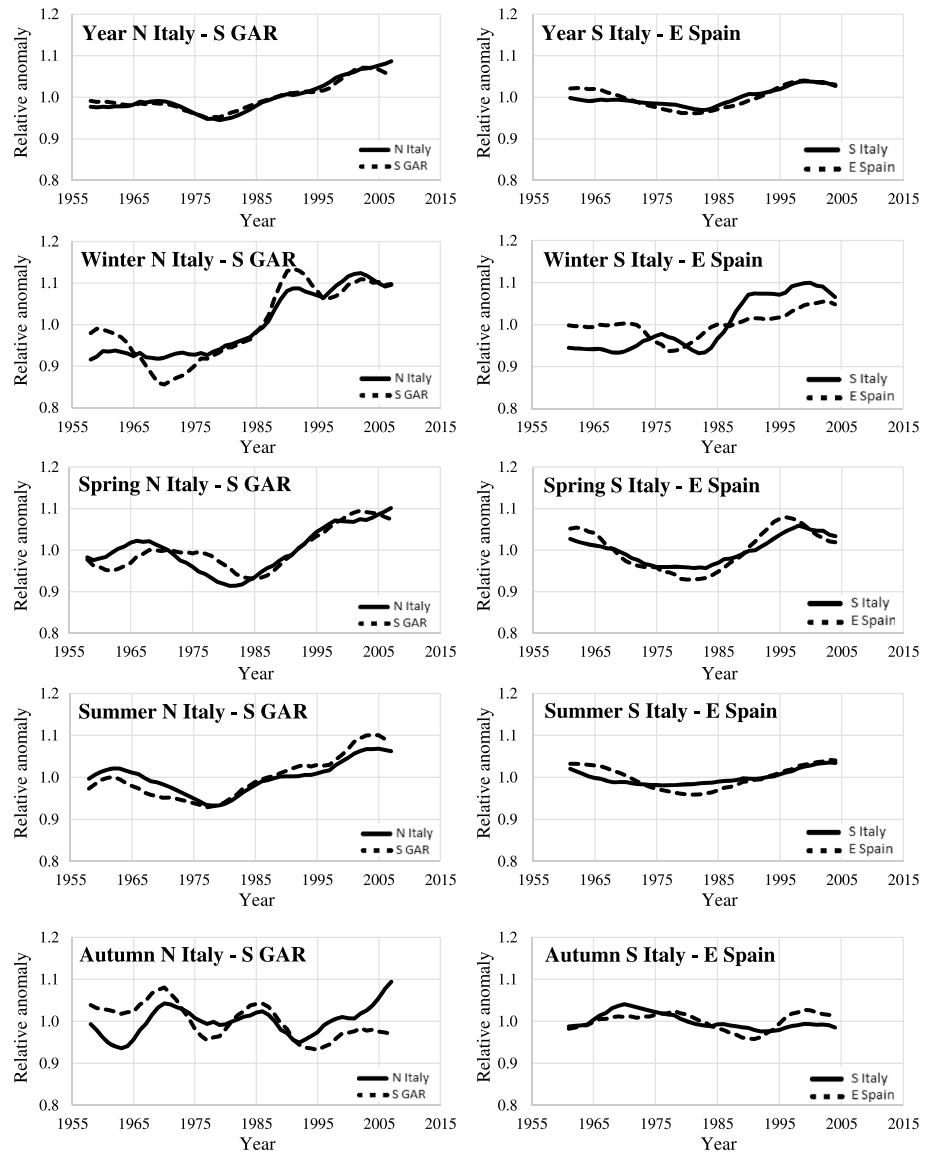


Figure 8. Sunshine duration low-pass filter annual and seasonal records for (left column) northern Italy and the southern part of the Greater Alpine Region (1958–2007 period) and for (right column) southern Italy and eastern Spain (1961–2004 period). The filter is the same as in Figure 6. All records are expressed in terms of relative anomalies from the 1958–2007/1961–2004 averages.

The agreement seems to be better for the subsequent brightening that seems to start both in southern Italy and in Spain at the beginning of the 1980s. Overall, there are no significant long-term trends since the 1960s in both southern Italy and eastern Spain series, unlike the clear tendency observed in northern Italy.

4.3. Comparison of Sunshine Duration Records With Total Cloud Cover Records

The comparison between TCC and SD records over Italy has been performed over the 1958–1995 period, using the data set of *Maugeri et al.* [2001], with data available until 1995. This data set contains only TCC data, whereas no information is available for cloud amount by low and middle clouds, which would be a better variable for investigating the cloudiness-SD relationship [e.g., *Xia*, 2010; *Matuszko*, 2012].

The TCC-SD comparison is shown in Figure 9 separately for northern and southern Italy, with all records expressed in terms of relative anomalies from the averages over the 1958–1995 period. Here, as well as in Figure 8, we show only the low-pass filter records.

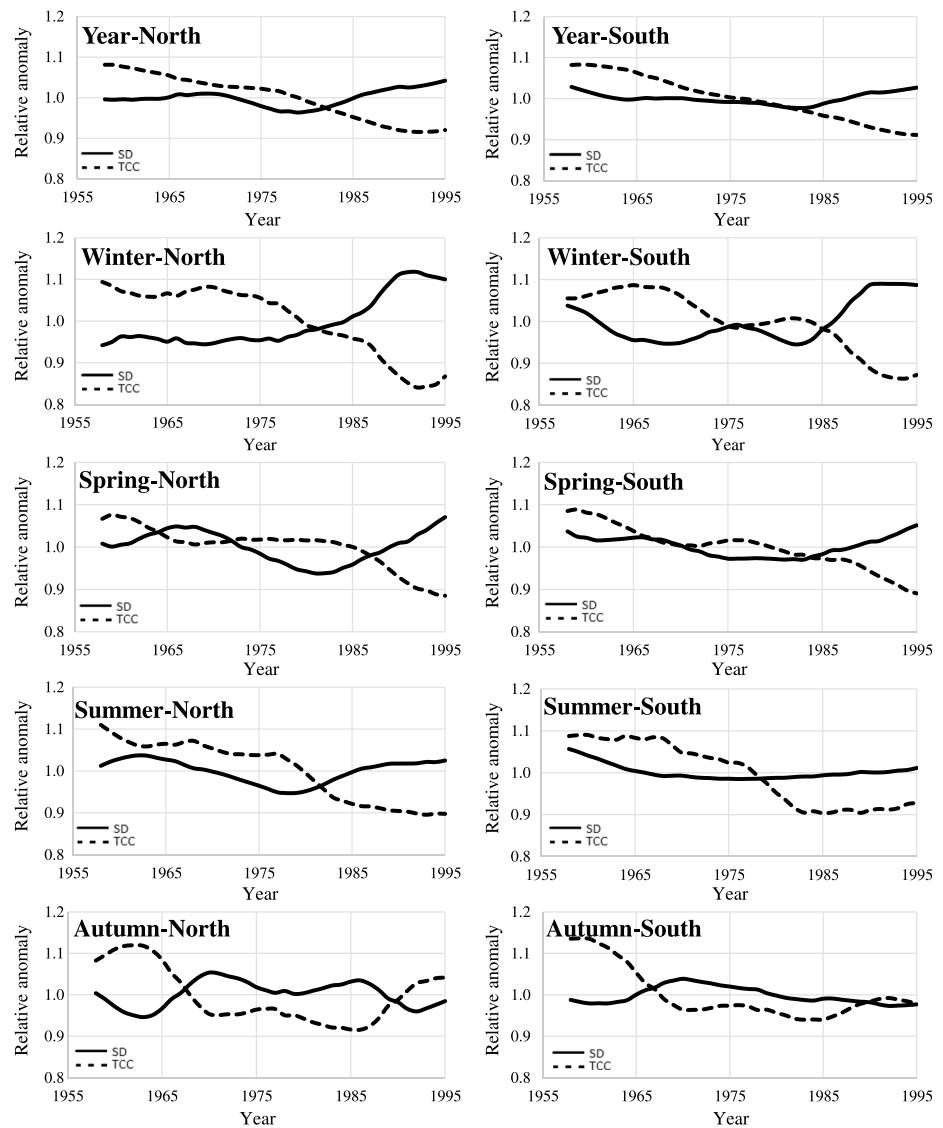


Figure 9. Sunshine duration (SD) and total cloud cover (TCC) low-pass filter annual and seasonal records (1958–1995) for (left column) northern and (right column) southern Italy. The filter is the same as in Figure 6. All records are expressed in terms of relative anomalies from the 1958–1995 averages.

The figure highlights that the negative correlation expected between SD and TCC is often not evident in the low-pass filter records. A clear example concerns the annual series in the period from about the beginning of 1960s to the beginning of the 1980s: here both SD and TCC have a decreasing tendency. This low-negative correlation, beside the annual records, is particularly evident in summer which shows very weak correlation also for the unfiltered records; the correlation coefficients for annual and summer records are, respectively, -0.53 and -0.55 for northern Italy and -0.39 and -0.54 for southern Italy. These results are in agreement with previous findings for Spain [Sanchez-Lorenzo *et al.*, 2009], which also highlight a disagreement between both variables from the 1960s to the mid-1980s, especially in summer months. On the contrary, if the residuals (relative deviations) from low-pass filter are considered, the negative correlation is much higher, with correlation coefficients ranging from -0.90 (spring) to -0.96 (autumn) for northern Italy and from -0.85 (summer) to -0.91 (spring) for southern Italy. This suggests the existence of different factors affecting the long-term tendencies in the two variables, as reported by Wang *et al.* [2012].

To highlight the role of TCC in driving SD, we created virtual SD annual and seasonal records using TCC as predictor, by exploiting the relationship between SD and TCC residuals: in particular, we evaluated the

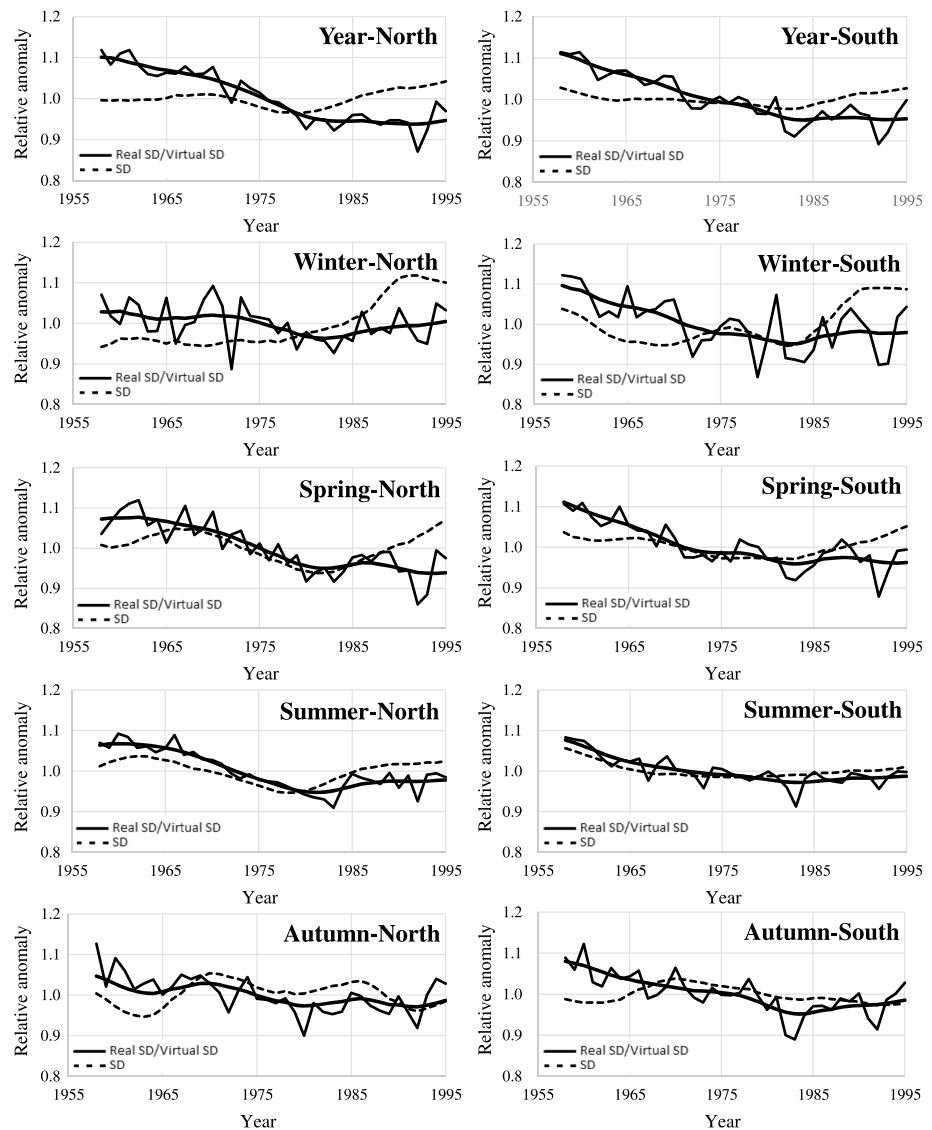


Figure 10. Continuous lines: ratios between the real sunshine duration (SD) anomalies and the virtual SD anomalies as predicted by total cloud cover anomalies for (left column) northern Italy and (right column) southern Italy. Heavy lines represent Gaussian low-pass filter (3 year standard deviation-11 year window) records. Dashed lines: real SD low-pass filter curves expressed as anomalies from the 1958–1995 means.

linear relationship between SD and TCC residuals and extended it to the real records. This linear relationship shows highest regression coefficients in winter (-0.92 ± 0.06 for northern Italy and -0.96 ± 0.09 for southern Italy) and spring (-0.90 ± 0.07 for northern Italy and -0.77 ± 0.06 for southern Italy), whereas in summer the regression coefficients are much lower (-0.45 ± 0.03 for northern Italy and -0.21 ± 0.02 for southern Italy).

Once we got these virtual SD records, we followed a technique suggested by other authors [e.g., Norris and Wild, 2007; Sanchez-Lorenzo et al., 2009] to remove the cloud effect from the real SD records and to detect whether there are signals linked to other factors than TCC. It consists in obtaining residual series by simply dividing the real SD records by the corresponding virtual SD records. These residual series should represent the SD tendency without the contribution due to TCC (i.e., keeping TCC constant). Results are shown in Figure 10. In order to give better evidence of the influence of TCC on SD, we also report in this figure the real SD low-pass filter curves (see Figure 6) that are here expressed in terms of anomalies with respect to the 1958–1995 means.

This figure shows a clear decrease from the end of the 1950s to the beginning of the 1980s (of about 15% at an annual scale) both in northern and southern Italy. This signal indicates that during this period there is an

important fraction of SD long-term evolution that cannot be explained by TCC: it must, therefore, depend on other factors such as changes in aerosol optical thickness, cloud properties, and/or water vapor content. The clear dimming caused by these factors has been partially masked, especially in northern Italy, by a strong TCC reduction. Therefore, the regional peculiarity of northern Italy—very low SD reduction in the dimming period—could simply be a consequence of a stronger decrease in TCC experienced by this region [Maugeri *et al.*, 2001]. After the beginning of the 1980s, the curves in Figure 10 do not show strong variations. Therefore, we can conclude that the effect of the other factors on SD becomes less relevant. The Italian brightening, at least up to 1995, seems therefore to be dominated by a TCC decrease.

It is also worth noting that the curves in Figure 10 have in most cases relevant minima in the periods 1982–1983 and 1992–1993. These pronounced minima, which have also been observed by other authors [Sanchez-Lorenzo *et al.*, 2009], might be a consequence of El Chichón (April 1982) and Pinatubo (June 1991) volcanic eruptions, which injected high amounts of sulfur dioxide (SO₂) into the stratosphere causing a worldwide reduction in direct solar radiation.

The results in Figure 10 are in reasonable agreement with anthropogenic emissions of pollutants and associated aerosol loads in the atmosphere over Europe [e.g., Streets *et al.*, 2006; Ruckstuhl and Norris, 2009; Smith *et al.*, 2011; Smith and Bond, 2014]. The agreement is good especially for the decrease between the beginning of the 1960s and the early 1980s, which corresponds to a strong increase in aerosol loads, whereas after 1980 the agreement is less evident as emissions and aerosol loads show a strong decrease that does not correspond to a clear increase of the curves in Figure 10. Anyway, the short period of Italy TCC records after the 1980s does not allow us better investigating this issue.

4.4. Sunshine Duration and Air Temperature

Global radiation can have a significant influence on temperature evolution at the Earth's surface [e.g., Wild *et al.*, 2007; Oldenborgh *et al.*, 2009; Philipona *et al.*, 2009; Wang and Dickinson, 2013]. It is, therefore, interesting to investigate whether the differences in the evolution of SD in northern and southern Italy correspond to differences in the evolution of air temperature.

Air temperature variability in Italy is discussed by Brunetti *et al.* [2006a] who analyzed a network of 67 secular records. Their results do not show relevant differences between northern and southern Italy. The same result is reported by Simolo *et al.* [2010] who analyzed 67 stations to study northern and southern Italy temperature trends (daily minimum and maximum temperatures— T_n and T_x) for the 1951–2008 period, showing rather low differences between northern and southern Italy seasonal and annual trends.

As a conclusion, the overall picture of air temperature in Italy does not give evidence of a strong link with the temporal evolution of SD: strong temperature trends are present also where SD trends are not present and important regional differences in SD trends do not correspond to significant differences in temperature trends. The lack of a strong SD effect on temperature long-term variability is probably caused by the fact that an increase in SD, besides producing an increase in daily maximum temperatures, produces a decrease in daily minimum values, linked to a reduction in cloudiness. This effect is also clear in very low correlation between Italian regional temperature and DTR records [Brunetti *et al.*, 2000].

5. Conclusions

A new data set of Italian quality checked sunshine duration records has been set up collecting data from different sources. The records have then been homogenized, completed, and projected onto a regular grid (1° × 1° resolution) covering the entire Italian territory and clustered into two main regions by means of a principal component analysis: northern Italy and southern Italy. The records of these areas were averaged in order to get the corresponding regional records for the 1936–2013 period.

The clearest feature of Italy sunshine duration records is an increasing tendency starting in the 1980s. Before this brightening signal, there is a decreasing tendency, which is, however, less evident than the more recent increasing trend, especially in northern Italy. In the early period, from middle of the 1930s to the 1950s, there is some evidence of an increasing tendency although this early brightening signal concerns a period in which data availability is very low, causing a greater uncertainty in regional records [Antón *et al.*, 2014]. The overall picture of Italian sunshine duration trends is, therefore, in reasonable agreement with the early

brightening-dimming-brightening phases observed in many areas of the world [Wild, 2009], even though some relevant regional peculiarities are evident especially in northern Italy.

Italian sunshine duration records turn out to be in good agreement with corresponding records from neighboring areas, specifically from the southern part of the Greater Alpine Region and from eastern Spain. This good agreement is both interesting, as it shows that sunshine duration exhibits a rather coherent signal over large regions, and useful, because it increases our confidence in the quality of records for Italy and neighboring regions.

The comparison of sunshine duration records with corresponding total cloud cover records shows that the expected negative correlation of these variables is often not evident as far as long-term tendencies are concerned [Wang *et al.*, 2012]. On the contrary, the residuals from the low-pass filter records show a very high negative correlation. This robust relationship was used here to separate the effect of cloud cover on sunshine duration from other factors. This separation suggests that during the global dimming period there is an important fraction of sunshine duration evolution that cannot be explained by total cloud cover. It must, therefore, depend on other factors as, for example, changes in aerosol optical thickness. Nevertheless, in Italy, especially in the northern region, the clear dimming caused by these other factors (e.g., aerosol optical thickness) has been partially masked by a strong reduction in total cloud cover. Therefore, the regional peculiarity of northern Italy—very low sunshine duration reduction in the dimming period—could simply be a consequence of a strong decrease in total cloud cover. Also, the strong brightening observed in Italy after the beginning of the 1980s is probably, at least up to 1995, dominated by a decrease in total cloud cover.

A more detailed understanding of the mechanism in Italy driving sunshine duration variability and trends calls for further research that should start with setting up a new cloudiness data set, which would extend the time period covered by the records considered in this paper and include the cloud amount by low and middle clouds. We plan to set up this data set in the near future. This new data set, together with a corresponding data set of daily temperature range records, will provide us with data to investigate a wider time interval and to study the relationship between SD, cloud cover, DTR [see e.g., Xia, 2013; Shen *et al.*, 2015], and aerosol load.

Acknowledgments

We sincerely thank all the institutions that allowed access to the data for research purposes and contributed to set up the 1936–2013 sunshine duration database. They are as follows (websites and contact persons are provided for data access): CRA-CMA (“Unità di ricerca per la climatologia e la meteorologia applicate all’agricoltura-Consiglio per la Ricerca e la Sperimentazione in Agricoltura.” The original data are available at <http://clima.entecra.it/homePage.htm> since 2003. The data of the previous years have to be requested at CRA-CMA) and Italian Air Force (“Servizio dell’Aeronautica Militare Italiana,” refer to <http://clima.meteoam.it/istruzioni.php> for data access). We received the data in the frame of an agreement between Italian Air Force and the Italian National Research Council, Luca Lombroso and Maurizio Ratti for the series of the Geophysical Observatory of Modena (<http://www.ossgeo.unimore.it>), and the series of the Meteorological Observatory of Pontremoli (“Osservatorio meteorologico Marsili”), Trieste, and Varese observatories (the Trieste original data are available online at <http://www.dst.univ.trieste.it/OM/ROM/>, the Varese data are available on request at “Centro Geofisico Prealpino-Società Astronomica G.V. Schiaparelli,” <http://www.astrgeo.va.it/>). The HISTALP data are available online in the HISTALP data set (<http://www.zamg.ac.at/histalp/>), the total cloud cover data come from Italian Air Force (“Servizio dell’Aeronautica Militare Italiana,” refer to <http://clima.meteoam.it/istruzioni.php> for data access), and, in conclusion, the Spanish data come from the Spanish Meteorological Agency (AEMET) (<http://www.aemet.es/es/portada>). We also kindly acknowledge Ruth Loewenstein for the help in improving the language of the paper. This study has been carried out in the framework of the EU project ECLISE (265240). A. Sanchez-Lorenzo was supported by the Postdoctoral Fellowships 2011-BP-B-00078 and JCI-2012-12508, and the Spanish Ministry of Science and Innovation Projects CGL2010-18546 and CGL2011-27574-C02-02.

References

- Aguiar, E., I. Auer, M. Brunet, T. C. Peterson, and J. Wieringa (2003), *Guidelines on Climate Metadata and Homogenization*, WMO-TD No. 1186, 52 pp., World Meteorological Organization, Geneva, Switzerland.
- Angell, J. K. (1990), Variation in United States cloudiness and sunshine duration between 1950 and the drought year of 1988, *J. Clim.*, *3*, 296–308, doi:10.1175/1520-0442(1990)003<0296:VIUSCA>2.0.CO;2.
- Ångström, A. (1924), Solar and terrestrial radiation, *Q. J. R. Meteorol. Soc.*, *50*(210), 121–126.
- Antón, M., J. M. Vaquero, and A. J. P. Aparicio (2014), The controversial early brightening in the first half of 20th century: A contribution from pyr heliometer measurements in Madrid (Spain), *Global Planet. Change*, *115*, 71–75, doi:10.1016/j.gloplacha.2014.01.013.
- Auer, I., *et al.* (2007), HISTALP-historical instrumental climatological surface time series of the Greater Alpine Region, *Int. J. Climatol.*, *27*, 17–46, doi:10.1002/joc.1377.
- Beltrano, M. C., G. Dal Monte, S. Esposito, and L. lafrate (2012a), The CRA-CMA archive and library for agricultural meteorology and phenology: A heritage to know, preserve and share, *Ital. J. Agrometeorol.*, *17*(3), 15–24.
- Beltrano, M. C., S. Esposito, and L. lafrate (2012b), The archive and library of the former Italian Central Office for Meteorology and Climatology, *Adv. Sci. Res.*, *8*, 58–65, doi:10.5194/asr-8-59-2012.
- Brzdil, R., A. A. Flocas, and H. S. Sahsamanoglou (1994), Fluctuation of sunshine duration in central and south-eastern Europe, *Int. J. Climatol.*, *14*, 1017–1034.
- Brunetti, M., L. Buffoni, M. Maugeri, and T. Nanni (2000), Trends of minimum and maximum daily temperatures in Italy from 1865 to 1996, *Theor. Appl. Climatol.*, *66*, 49–60.
- Brunetti, M., M. Maugeri, F. Monti, and T. Nanni (2006a), Temperature and precipitation variability in Italy in the last two centuries from homogenized instrumental time series, *Int. J. Climatol.*, *26*(3), 345–381, doi:10.1002/joc.1251.
- Brunetti, M., M. Maugeri, T. Nanni, I. Auer, R. Böhm, and W. Schöner (2006b), Precipitation variability and changes in the Greater Alpine Region over the 1800–2003 period, *J. Geophys. Res.*, *111*, D11107, doi:10.1029/2005JD006674.
- Brunetti, M., G. Lentini, M. Maugeri, T. Nanni, I. Auer, R. Böhm, and W. Schöner (2009), Climate variability and change in the Greater Alpine Region over the last two centuries based on multi-variable analysis, *Int. J. Climatol.*, *29*(15), 2197–2225, doi:10.1002/joc.1857.
- Brunetti, M., M. Maugeri, T. Nanni, C. Simolo, and J. Spinoni (2013), High-resolution temperature climatology for Italy: Interpolation method intercomparison, *Int. J. Climatol.*, *34*(4), 1278–1296, doi:10.1002/joc.3764.
- Chiachio, M., and M. Wild (2010), Influence of NAO and clouds on long-term seasonal variations of surface solar radiation in Europe, *J. Geophys. Res.*, *115*, D00D22, doi:10.1029/2009JD012182.
- Craddock, J. M. (1979), Methods of comparing annual rainfall records for climatic purposes, *Weather*, *34*(9), 332–346, doi:10.1002/j.1477-8696.1979.tb03465.x.
- Goldberg, B., and W. H. Klein (1971), Comparison of normal incident solar energy measurements at Washington, D. C., *Sol. Energy*, *13*, 311–321.
- Hartmann, D. L., V. Ramanathan, A. Berroir, and G. E. Hunt (1986), Earth radiation budget data and climate research, *Rev. Geophys.*, *24*(2), 439–468, doi:10.1029/RG024i002p00439.

- Italian Air Force (2012), La radiazione solare globale e la durata del soleggiamento in Italia dal 1991 al 2010, Aeronautica Militare, Reparto di Sperimentazioni di Meteorologia Aeronautica.
- Jones, P. A., and A. Henderson-Sellers (1992), Historical records of cloudiness and sunshine in Australia, *J. Clim.*, *5*, 260–267, doi:10.1175/1520-0442(1992)005<0260:HROCAS>2.0.CO;2.
- Kaiser, D. P., and Y. Qian (2002), Decreasing trends in sunshine duration over China for 1954–1998: Indication of increased haze pollution?, *Geophys. Res. Lett.*, *29*(21), 2042, doi:10.1029/2002GL016057.
- Kitsara, G., G. Papaioannou, A. Papathanasiou, and A. Retalis (2013), Dimming/brightening in Athens: Trends in sunshine duration, cloud cover and reference evapotranspiration, *Water Resour. Manage.*, *27*, 1623–1633, doi:10.1007/s11269-012-0229-4.
- Liang, F., and X. A. Xia (2005), Long-term trends in solar radiation and the associated climatic factors over China for 1961–2000, *Ann. Geophys.*, *23*(7), 2425–2432, doi:10.5194/angeo-23-2425-2005.
- Liepert, B. G. (2002), Observed reductions of surface solar radiation at sites in the United States and worldwide from 1961 to 1990, *Geophys. Res. Lett.*, *29*(10), 1421, doi:10.1029/2002GL014910.
- Lohmann, U., and J. Feichter (2005), Global indirect aerosol effects: A review, *Atmos. Chem. Phys.*, *5*, 715–737, doi:10.5194/acp-5-715-2005.
- Lombroso, L., and S. Quattrocchi (2008), *L'Osservatorio di Modena: 180 Anni di Misure Meteorologiche*, Società Meteorologica Subalpina, Castello Borello, Bussoletto (TO), Italy.
- Magee, B. N., E. Melaas, P. M. Finocchio, M. Jardel, A. Noonan, and M. J. Iacono (2014), Blue hill observatory sunshine: Assessment of climate signals in the longest continuous meteorological record in North America, *Bull. Am. Meteorol. Soc.*, doi:10.1175/BAMS-D-12-00206.1.
- Martínez-Lozano, J. A., F. Tena, J. E. Onrubia, and J. De La Rubia (1984), The historical evolution of the Ångström formula and its modifications: Review and bibliography, *Agric. For. Meteorol.*, *33*(2–3), 109–128.
- Matuszko, D. (2012), Influence of cloudiness on sunshine duration, *Int. J. Climatol.*, *32*, 1527–2536, doi:10.1002/joc.2370.
- Matuszko, D. (2014), Long-term variability in solar radiation in Krakow based on measurements of sunshine duration, *Int. J. Climatol.*, *34*, 228–234, doi:10.1002/joc.3681.
- Maugeri, M., Z. Bagnati, M. Brunetti, and T. Nanni (2001), Trends in Italian total cloud amount, 1951–1996, *Geophys. Res. Lett.*, *28*(24), 4551–4554, doi:10.1029/2001GL013754.
- Nabat, P., S. Somot, M. Mallet, A. Sanchez-Lorenzo, and M. Wild (2014), Contribution of anthropogenic sulfate aerosols to the changing Euro-Mediterranean climate since 1980, *Geophys. Res. Lett.*, *41*, 5605–5611, doi:10.1002/2014GL060798.
- New, M., M. Hulme, and P. D. Jones (2000), Representing twentieth-century space-time climate variability. Part II: Development of 1901–96 monthly grids of terrestrial surface climate, *J. Clim.*, *13*, 2217–2238.
- Norris, J. R., and M. Wild (2007), Trends in aerosol radiative effects over Europe inferred from observed cloud cover, solar “dimming,” and solar “brightening”, *J. Geophys. Res.*, *112*, D08214, doi:10.1029/2006JD007794.
- Ohmura, A. (2009), Observed decadal variations in surface solar radiation and their causes, *J. Geophys. Res.*, *114*, D00D05, doi:10.1029/2008JD011290.
- Ohmura, A., and H. Gilgen (1993), Re-evaluation of the global energy balance, in *Interactions Between Global Climate Subsystems the Legacy of Hann*, edited by G. A. McBean, and M. Hantel, pp. 93–110, AGU, Washington, D. C., doi:10.1029/GM075p0093.
- Ohmura, A., and H. Lang (1989), Secular variation of global radiation in Europe, in *IRS'88: Current Problems in Atmospheric Radiation*, edited by J. Lenoble and J.-F. Geleyn, pp. 298–301, A. Deepak, Hampton, Va.
- Oldenborgh, G. J., S. Drijfhout, A. van Ulden, R. Haarsma, A. Sterl, C. Severijns, W. Hazeleger, and H. Dijkstra (2009), Western Europe is warming much faster than expected, *Clim. Past*, *5*, 1–12.
- Philipona, R., K. Behrens, and C. Ruckstuhl (2009), How declining aerosols and rising greenhouse gases forced rapid warming in Europe since the 1980s, *Geophys. Res. Lett.*, *36*, L02806, doi:10.1029/2008GL036350.
- Preisendorfer, R. W. (1988), *Principal Component Analysis in Meteorology and Oceanography*, 425 pp., Elsevier, New York.
- Prescott, J. A. (1940), Evaporation from a water surface in relation to solar radiation, *Trans. R. Soc. South Aust.*, *64*, 114–118.
- Rahimzadeh, F., A. Sanchez-Lorenzo, M. Hamed, M. Kruk, and M. Wild (2014), New evidence on the dimming/brightening phenomenon and decreasing diurnal temperature range in Iran (1961–2009), *Int. J. Climatol.*, doi:10.1002/joc.4107, in press.
- Raichijk, C. (2012), Observed trends in sunshine duration over South America, *Int. J. Climatol.*, *32*, 669–680, doi:10.1002/joc.2296.
- Ramanathan, V., P. J. Crutzen, J. T. Kiehl, and D. Rosenfeld (2001), Aerosol, climate, and the hydrological cycle, *Science*, *294*(5549), 2119–2124, doi:10.1126/science.1064034.
- Ratti, M. (2010), Il clima del 2010 a Pontremoli: Temperature quasi normali e piovosità straordinaria, Società meteorologica italiana, Nimbus. [Available at <http://www.nimbus.it/clima/2010/110204PontremoliClima2010.htm>.]
- Rosenfeld, D., et al. (2014), Global observations of aerosol-cloud-precipitation-climate interactions, *Rev. Geophys.*, *52*, 750–808, doi:10.1002/2013RG000441.
- Ruckstuhl, C., and J. R. Norris (2009), How do aerosol histories affect solar “dimming” and “brightening” over Europe?: IPCC-AR4 models versus observations, *J. Geophys. Res.*, *114*, D00D04, doi:10.1029/2008JD011066.
- Ruckstuhl, C., et al. (2008), Aerosol and cloud effects on solar brightening and the recent rapid warming, *Geophys. Res. Lett.*, *35*, L12708, doi:10.1029/2008GL034228.
- Russak, V. (1990), Trends of solar radiation, cloudiness and atmospheric transparency during recent decades in Estonia, *Tellus, Ser. B*, *42*, 206–210.
- Sanchez-Lorenzo, A., and M. Wild (2012), Decadal variations in estimated surface solar radiation over Switzerland since the late 19th century, *Atmos. Chem. Phys.*, *12*, 8635–8644, doi:10.5194/acp-12-8635-2012.
- Sanchez-Lorenzo, A., M. Brunetti, J. Calbò, and J. Martin-Vide (2007), Recent spatial and temporal variability and trends of sunshine duration over the Iberian Peninsula from a homogenized data set, *J. Geophys. Res.*, *112*, D20115, doi:10.1029/2007JD008677.
- Sanchez-Lorenzo, A., J. Calbò, and J. Martin-Vide (2008), Spatial and temporal trends in sunshine duration over Western Europe (1938–2004), *J. Clim.*, *21*, 6089–6098, doi:10.1175/2008JCLI2442.1.
- Sanchez-Lorenzo, A., J. Calbò, M. Brunetti, and C. Deser (2009), Dimming/brightening over the Iberian Peninsula: Trends in sunshine duration and cloud cover and their relations with atmospheric circulation, *J. Geophys. Res.*, *114*, D00D09, doi:10.1029/2008JD011394.
- Sanchez-Lorenzo, A., J. Calbò, and M. Wild (2013a), Global and diffuse solar radiation in Spain: Building a homogeneous dataset and assessing their trends, *Global Planet. Change*, *100*, 343–352, doi:10.1016/j.gloplacha.2012.11.010.
- Sanchez-Lorenzo, A., J. Calbò, M. Wild, C. Azorin-Molina, and A. Sánchez-Romero (2013b), New insights into the history of the Campbell-Stokes sunshine recorder, *Weather*, *68*(12), 327–331, doi:10.1002/wea.2130.
- Sanchez-Lorenzo, A., M. Wild, and J. Trentmann (2013c), Validation and stability assessment of the monthly mean CM SAF surface solar radiation dataset over Europe against a homogenized surface dataset (1983–2005), *Remote Sens. Environ.*, *134*, 355–366, doi:10.1016/j.rse.2013.03.012.

- Sanchez-Romero, A., A. Sanchez-Lorenzo, J. Calbó, J. A. González, and C. Azorin-Molina (2014), The signal of aerosol induced changes in sunshine duration records: A review of the evidence, *J. Geophys. Res. Atmos.*, *119*, 4657–4673, doi:10.1002/2013JD021393.
- Shen, X., B. Liu, G. Li, Z. Wu, Y. Jin, P. Yu, and D. Zhou (2015), Spatiotemporal change of diurnal temperature range and its relationship with sunshine duration and precipitation in China, *J. Geophys. Res. Atmos.*, *119*, 13,163–13,179, doi:10.1002/2014JD022326.
- Simolo, C., M. Brunetti, M. Maugeri, T. Nanni, and A. Speranza (2010), Understanding climate change-induced variations in daily temperature distributions over Italy, *J. Geophys. Res.*, *115*, D22110, doi:10.1029/2010JD014088.
- Smith, S. J., and T. C. Bond (2014), Two hundred fifty years of aerosols and climate: The end of the age of aerosols, *Atmos. Chem. Phys.*, *14*, 537–549, doi:10.5194/acp-14-537-2014.
- Smith, S. J., J. van Aardenne, Z. Klimont, R. J. Andres, A. Volke, and S. Delgado Arias (2011), Anthropogenic sulfur dioxide emission: 1850–2005, *Atmos. Chem. Phys.*, *11*, 1101–1116, doi:10.5194/acp-11-1101-2011.
- Sneyers, R. (1992), On the use of statistical analysis for the objective determination of climatic change, *Meteorol. Z.*, *1*(5), 247–256.
- Soni, V. K., G. Pandithurai, and D. S. Pai (2012), Evaluation of long-term changes of solar radiation in India, *Int. J. Climatol.*, *32*, 540–551, doi:10.1002/joc.2294.
- Spinoni, J., M. Brunetti, M. Maugeri, and C. Simolo (2012), 1961–1990 monthly high-resolution solar radiation climatologies for Italy, *Adv. Sci. Res.*, *8*, 19–25, doi:10.5194/asr-8-19-2012.
- Stanhill, G. (2005), Global dimming: A new aspect of climate change, *Weather*, *60*(1), 11–14, doi:10.1256/wea.210.03.
- Stanhill, G. (2007), A perspective on global warming, dimming, and brightening, *Eos Trans. AGU*, *88*(5), 58–59, doi:10.1029/2007EO050007.
- Stanhill, G., and S. Cohen (2001), Global dimming: A review of the evidence for a widespread and significant reduction in global radiation with discussion of its probable causes and possible agricultural consequences, *Agric. For. Meteorol.*, *107*, 255–278, doi:10.1016/S0168-1923(00)00241-0.
- Stanhill, G., and S. Cohen (2005), Solar radiation changes in United States during the twentieth century: Evidence from sunshine duration measurements, *J. Clim.*, *18*, 1503–1512, doi:10.1175/JCLI3354.1.
- Stanhill, G., and S. Cohen (2008), Solar radiation changes in Japan during the 20th century: Evidence from sunshine duration measurements, *J. Meteorol. Soc. Jpn.*, *86*(1), 57–67, doi:10.2151/jmsj.86.57.
- Stanhill, G., and S. Moreshet (1992), Global radiation climate changes: The world network, *Clim. Change*, *21*, 57–75, doi:10.1007/BF00143253.
- Stravisi, F. (2004), Dati orari di eliofania: Trieste 1886–2003, *Rap n°104, OM 04/6*, Università degli Studi di Trieste-Dipartimento di Scienze della Terra.
- Streets, D. G., Y. Wu, and M. Chin (2006), Two-decadal aerosol trends as a likely explanation of the global dimming/brightening transition, *Geophys. Res. Lett.*, *33*, L15806, doi:10.1029/2006GL026471.
- Suraqui, S., H. Tabor, W. H. Klein, and B. Goldberg (1974), Solar radiation changes at Mt. St. Katherine after forty years, *Sol. Energy*, *16*, 155–158.
- Von Storch, H. (1995), Spatial patterns: EOFs and CCA, in *Analysis of Climate Variability: Applications of Statistical Techniques*, edited by H. von Storch, and A. Navarra, pp. 227–258, Springer, New York, doi:10.1007/978-3-662-03167-4_13.
- Wang, K. (2014), Measurement biases explain discrepancies between the observed and simulated decadal variability of surface incident solar radiation, *Sci. Rep.*, *4*, 6144, doi:10.1038/srep06144.
- Wang, K., and R. Dickinson (2013), Contribution of solar radiation to decadal temperature variability over land, *Proc. Natl. Acad. Sci. U.S.A.*, *110*(37), 14,877–14,882, doi:10.1073/pnas.1311433110.
- Wang, K., R. E. Dickinson, Q. Ma, J. A. Augustine, and M. Wild (2013), Measurement methods affect the observed global dimming and brightening, *J. Clim.*, *26*, 4112–4120, doi:10.1175/JCLI-D-12-00482.1.
- Wang, K. C., R. E. Dickinson, M. Wild, and S. Liang (2012), Atmospheric impacts on climatic variability of surface incident solar radiation, *Atmos. Chem. Phys.*, *12*, 9581–9592, doi:10.5194/acp-12-9581-2012.
- Wang, Y. W., and Y. H. Yang (2014), China's dimming and brightening: Evidence, causes and hydrological implications, *Ann. Geophys.*, *32*, 41–55, doi:10.5194/angeo-32-41-2014.
- Wild, M. (2005), From dimming to brightening: Decadal changes in solar radiation at Earth's surface, *Science*, *308*, 847, doi:10.1126/science.1103215.
- Wild, M. (2009), Global dimming and brightening: A review, *J. Geophys. Res.*, *114*, D00D16, doi:10.1029/2008JD011470.
- Wild, M. (2012), Enlightening global dimming and brightening, *Bull. Am. Meteorol. Soc.*, *93*, 27–37, doi:10.1175/BAMS-D-11-00074.1.
- Wild, M., A. Ohmura, H. Gilgen, and D. Rosenfeld (2004), On the consistency of trends in radiation and temperature records and implications for the global hydrological cycle, *Geophys. Res. Lett.*, *31*, L11201, doi:10.1029/2003GL019188.
- Wild, M., H. Gilgen, A. Roesch, A. Ohmura, C. N. Long, E. G. Dutton, B. Forgan, A. Kallis, V. Russak, and A. Tsvetkov (2005), From dimming to brightening: Decadal changes in surface solar radiation at Earth's surface, *Science*, *308*(5723), 847–850, doi:10.1126/science.1103215.
- Wild, M., A. Ohmura, and K. Makowski (2007), Impact of global dimming and brightening on global warming, *Geophys. Res. Lett.*, *34*, L04702, doi:10.1029/2006GL028031.
- Wild, M., B. Trüssel, A. Ohmura, C. N. Long, G. König-Langlo, E. G. Dutton, and A. Tsvetkov (2009), Global dimming and brightening: An update beyond 2000, *J. Geophys. Res.*, *114*, D00D13, doi:10.1029/2008JD011382.
- Wild, M., D. Folini, C. Schaer, N. Loeb, E. G. Dutton, and G. König-Langlo (2013), The global energy balance from a surface perspective, *Clim. Dyn.*, *40*, 3107–3134, doi:10.1007/s00382-012-1569-8.
- Wilks, D. S. (1995), *Statistical Methods in the Atmospheric Sciences*, *Int. Geophys. Ser.*, vol. 59, 2nd ed., 464 pp., Academic Press, New York.
- WMO-No.8 (1969), Solar radiation and sunshine duration, in *Guide to Meteorological Instruments and Observing Practices*, 3rd ed., chap. 9, World Meteorological Organization, Geneva, Switzerland.
- WMO-No.8 (2008), Measurement of sunshine duration, in *Guide to Meteorological Instruments and Methods of Observation*, chap. 8, World Meteorological Organization, Geneva, Switzerland.
- Xia, X. (2010), Spatiotemporal changes in sunshine duration and cloud amount as well as their relationship in China during 1954–2005, *J. Geophys. Res.*, *115*, D00K06, doi:10.1029/2009JD012879.
- Xia, X. (2013), Variability and trend of diurnal temperature range in China and their relationship to total cloud cover and sunshine duration, *Ann. Geophys.*, *31*, 795–804, doi:10.5194/angeo-31-795-2013.